ELSEVIER

# Novel Cement Matrices by Accelerated Hydration of the Ferrite Phase in Portland Cement via Chemical Activation: Kinetics and Cementitious Properties

Wolfgang Schwarz
*Holderbank Management & Consulting Ltd., Holderbank, Switzerland*

*The effects of the admixture of potassium citrate and potassium carbonate to portland cement with and without gypsum on the kinetics of the dissolution of the clinker phases, formation of hydration products, and cementitous properties in ISO-mortar and concrete were investigated. Quantitative X-ray diffraction (QXRD) data indicate that the admixture of citrate to portland cements increases the dissolution rate of the ferrite phase. In the presence of 1 to 3% potassium citrate, the ferrite phases dissolve nearly completely within 6 hours. Citrate is assumed to act via surface complexation and ligand-promoted dissolution. Set and hardening coincides with the formation of AFm phases. Semiquantitative background evaluation of XRD spectra indicates that citrate promotes the formation of noncrystalline phases, in which iron(III)hydroxide presumably forms the polymeric backbone whereas carbonate stabilizes crystalline AFm areas. Optimum early strength in ISO-mortar and concrete is correlated with the formation of crystalline and noncrystalline phases.* ADVANCED CEMENT BASED MATERIALS 1995, 2, 189–200

**KEY WORDS:** AFm, AFt, Calcium carbo aluminate hydrate, Citric acid, Crystalline phases, Ettringite, Ferrite, Gypsum free cement, High early strength, Iron(III) complexation, Lignosulfonate, Noncrystalline phases, Portland cement, Potassium carbonate, Rapid hardening

The principal constituents of normal Portland cement are calcium silicates, calcium-aluminates, calcium-ferro-aluminates, and gypsum. Except for dicalcium silicate (belite), the anhydrous clinker phases are highly reactive towards water. When mixed together in Portland cement, a significant alteration of their reactivity and of the course of their hydration is observed [1–3], especially for the ferro-aluminate phases [4]. The chemical and physical properties of the hardened cement paste are understood in terms of the principal hydrous products—ettringite, calcium-silicate-hydrate (C-S-H), and portlandite—formed during the hydration of aluminate and alite. The reactivity of Portland cement can be regulated either by accelerating and retarding admixtures or by modifying the alite and aluminate content of the clinker. The ferrite phase is regarded as the least reactive phase, yielding similar hydration products as the aluminate phase [1,2]. Its role as a strength-building phase and its contribution to the cementitious properties is still controversial, but a significant contribution of the ferrite phase to late strength was reported [5]. Recently, increased later age strength obtained by the admixture of triisopropanolamine was attributed by Gartner [6] to the enhanced hydration of the ferrite phase due to Fe(III) complexation. In this paper, results of the influence of activating admixtures on the kinetics of the dissolution of the clinker phases, especially the ferrite phase, and of the formation of hydrous products and their influence on cementitious properties are reported.

## Experimental

### Materials

**RAW MATERIALS.** Two types of clinker (Table 1) were used for the preparation of cement mixes: clinker (Blaine 4390 $cm^2/g$) used for ordinary Portland cement (OPC) production and a $C_3A$-free clinker (Blaine 5070 $cm^2/g$) used for the production of sulfate-resistant portland cements. The reference cements were prepared by mixing ground clinker with the appropriate amount of gypsum. For the preparation of the cement mixtures, ground clinker instead of commercial Portland cement

Address correspondence to: Wolfgang Schwarz, Institute for Building Materials, ETH-Zurich/HIL, CH-8093 Zurich, Switzerland.
Received May 21, 1994; Accepted February 14, 1995



ISSN 1065-7355/95/$9.50
SSDI 1065-7355(95)00018-M

Advn Cem Bas Mat
1995;2:189–200

**TABLE 1.** Clinker composition

| Clinker | Component Oxides (mass%) | | | | | | | | | | | Other (mass%) | | |
|---|---|---|---|---|---|---|---|---|---|---|---|---|---|---|
| | $SiO_2$ | $Al_2O_3$ | $Fe_2O_3$ | CaO | MgO | $SO_3$ | $K_2O$ | $Na_2O$ | $TiO_2$ | $Mn_2O_3$ | $P_2O_5$ | LOI | Sum | $CaO_{free}$ |
| 1 | 21.1 | 3.2 | 7.0 | 64.9 | 0.78 | 1.1 | 0.58 | 0.35 | 0.17 | 0.03 | 0.08 | 0.29 | 99.6 | 1.2 |
| 2 | 22.7 | 4.9 | 2.8 | 64.4 | 1.6 | 1.3 | 1.1 | 0.30 | 0.22 | 0.05 | 0.17 | 0.28 | 99.8 | 1.1 |

| | Phase Composition (mass%) | | | | | | | Specific Weight ($g/cm^3$) | Fineness Blaine ($m^2/kg$) |
|---|---|---|---|---|---|---|---|---|---|
| | Alite | Belite | $C_3A$ | Ferrite | $CaO_{free}$ | Periclase | Alkali-sulfate | | |
| 1 | 65.6 | 13.9 | 0.3 | 17.6 | 1.2 | 0.0 | 1.9 | 3.25 | 507 |
| 2 | 53.8 | 29.3 | 4.0 | 8.4 | 1.6 | 0.1 | 2.8 | 3.27 | 439 |

Clinker phases were determined by microscopic point counting. LOI = loss on ignition.

was used to eliminate calcium-sulfate-hydrate phases as additional nonspecified variables.

The gypsum used was a commercial high quality ground gypsum (90% <60 μm). The additives, coarse caustic potassium carbonate and tripotassium citrate monohydrate, were commercially available technical grade products.

**CEMENT PASTES.** The cements (Table 2) were prepared by mixing the ground clinkers with the additives and with the required amounts of gypsum in a laboratory mixer. The reference cement pastes were prepared with a water:cement ratio of 0.38, the cement pastes of the series with clinker 1 (1-PG, 1-CG, 1-PCG) were prepared with a water:cement ratio of 0.26, and the cement paste samples of series 2 (2-PCG and 2-GfC) were prepared with a water:cement ratio of 0.38.

The cement paste samples were stored in polycarbonate forms under air, saturated with water, for 24 hours. The hardened cement paste prisms were demolded at the required sampling time. Seven-day and 28-day samples were demolded after 24 hours and stored under water at ambient temperature.

X-ray diffraction (XRD) samples were prepared by crushing and pregrinding the specimen under acetone and by grinding 2 g samples in a Retsch-micromill. Further hydration was stopped with acetone and by redrying under vacuum for about 15–30 minutes.

## XRD Studies

**QXRD PATTERNS OF HYDRATED SAMPLES.** The powdered samples were compacted under vibration, and the sample holder was rotated at 30 rpm during measurement. The XRD patterns were recorded with a Siemens D500TT diffractometer. Parameters are reported elsewhere [7]. The integral intensities and the mass-absorption coefficients, calculated from chemical analytical data and the losses of ignition (LOIs), were used for the quantitative evaluation following the method of Klug and Alexander [8]. Clinker phases of the reference samples 1-REF and 2-REF, determined by microscopic phase counting, were used as external standards.

The clinker phase contents are calculated in weight percent, referring to the LOI-free samples. The amount of portlandite was calculated by using an external portlandite standard, and values were verified with data from thermo-gravimetric measurements on admixture-free reference samples.

**IN SITU HYDRATION.** Pastes were prepared with sufficient water (w:c = 0.38 for the reference, w:c = 0.24 for 1-PCG, and w:c = 0.27 for 2-PCG-pastes) to make them fluid but to avoid bleeding. The pastes were placed in a 27 × 2 mm sample holder and covered with a 1 μm thick stretched polypropylene film. The XRD patterns were recorded continuously over the scan range 8–53° 2θ, counting time was 1.6 seconds, recording time for each run was 65 minutes.

**EVALUATION OF THE BACKGROUND.** The background in XRD patterns is composed of very broad reflections from noncrystalline materials with contributions from poorly crystallized and microcrystalline materials due to line broadening and from non-Bragg scattering effect [7]. To obtain information about the nature of the

**TABLE 2.** Cement mix characteristics

| Cement* | 1-REF | 1-PCG | 1-PC | 1-CG | 1-PG | 1-GFC | 2-REF | 2-PCG | 2-CG | 2-GFC |
|---|---|---|---|---|---|---|---|---|---|---|
| $K_2CO_3$ | — | 1.85 | 1.85 | — | 3.00 | 3.00 | — | 1.85 | — | 3.00 |
| $K_3$-citrate | — | 2.70 | 2.70 | 2.70 | — | — | — | 2.70 | 2.70 | — |
| Na-Lignosulfonate | — | — | — | — | — | 0.60 | — | — | — | 0.60 |
| Gypsum | 1.00 | 1.00 | — | 1.00 | 1.00 | — | 4.00 | 4.00 | 4.00 | — |

1- denotes series with clinker 1; 2- denotes series with clinker 2.
*Weight % per weight clinker.

noncrystalline phases, the underlying background of the XRD patterns recorded from quantitative XRD (QXRD) samples was fitted with narrow parabolas excluding as far as possible tails from the superposed XRD lines. The width of the parabolas was chosen such that crystalline material >50 Å was excluded. This is possible only to a limited extent due to the complexity of the XRD patterns allowing only qualitative evaluation.

By fitting the XRD background with very broad parabolas, contributions from microcrystalline and poorly crystallized materials can be excluded. The integral intensity of the fitted background was quantitatively determined on 30-minute to 28-day-old samples and taken as a measure of the noncrystalline part of the sample. The corresponding measure of the crystalline part was obtained by subtracting the integral intensity of the background from the total integral intensity of the XRD spectrum between 8° and 53° 2θ. These values were corrected for the non-Bragg background by subtracting the background of the corresponding 30-minute-old samples.

**CHARACTERISATION OF CEMENTITIOUS PROPERTIES IN ISO-MORTAR AND CONCRETE.** ISO-mortar was prepared according to ISO 772 (ENV-196). Water:cement ratios were chosen to obtain fluid (140–160%), standard (110%), and stiff (90–100%) mortars. Flow in percent was determined according to ASTM C 230-83. Strength was measured on 40 × 40 × 160 mm prisms. Setting times were determined on mortar with a Vicat needle.

Concrete mixes were prepared in batches of 75 L with 0/32 mm standard dry aggregate: 2-PCG-cement, 400 kg/m$^3$; sand (0/5 mm), 756 kg/m$^3$; coarse aggregate (5/32 mm), 1182 kg/m$^3$; water, 148 kg/m$^3$; air content (%), 0.9; slump after 30 minutes (cm), 19/18; flow (cm), 45–50; fresh concrete density (kg/m$^3$), 2,455.

Mixing time was 3.5 minutes. The flow was measured according to DIN 1048/1; slump was measured according to ASTM C 143-78. Strength was tested on 12 × 12 × 36 cm prisms. Set was determined on the concrete prisms.

# Results

## *Dissolution of Clinker Phases*

The influence of potassium carbonate and potassium citrate on the rate of the dissolution of clinker phases and on the formation of hydrous products in cement pastes was determined by quantitative and qualitative evaluation of XRD patterns. The setting times were adjusted within a range of 30–90 minutes by the amount of gypsum or lignosulfonate (gfc formulations) added.

**DISSOLUTION OF THE FERRITE AND ALUMINATE PHASES.** The QXRD results of the early hydration are given in the Figures 1 and 2, and results of the late hydration are given in Table 3. Both potassium carbonate and potassium citrate accelerate the initial rate of dissolution of the ferrite phase in comparison with the reference sample to approximately 50% and 80% dissolution, respectively. In the presense of citrate (1-CG) and in combination with carbonate (1-PCG), the ferrite dissolution proceeds at equal rate during early hydration, but further ferrite dissolution is enhanced during late hydration (Table 3). The residual ferrite after 28 days is attributed to inclusions in agglomerated unreacted alite particles [7,9]. With regard to the accelerating effect of alkalis on the dissolution of clinker phases, especially aluminates [1,3], the amount of admixtures added was chosen such that in all samples approximately the same amount of potassium was added (2.0–2.4 wt% $K_2O$), except in the 1-CG sample (1.18 wt% $K_2O$). Despite the difference in the $K_2O$ contents in the 1-CG and 1-PCG samples, the rate of ferrite dissolution is about equal. From this, it is concluded that potassium has no significant influence on the dissolution rate of the ferrite phase in the presence of citrate.

In the presence of potassium carbonate and potassium citrate (2-PCG), the dissolution of both aluminate and ferrite is accelerated (Figure 2). In the potassium carbonate- and lignosulfonate-containing cement

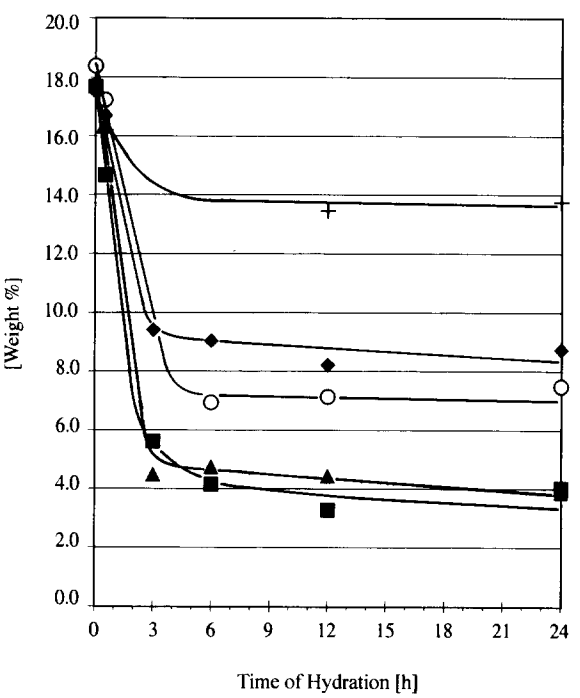


**FIGURE 1.** Influence of potassium carbonate (1-GfC, 1-PG), potassium citrate (1-CG), and potassium carbonate and potassium citrate (1-PCG) on the rate of ferrite dissolution at w:c = 0.26 during early hydration in comparison with the reference at w:c = 0.38. ○, 1-GfC; ◆, 1-PG; ▲, 1-CG; ■, 1-PCG; +, 1-REF.

Advn Cem Bas Mat
1995;2:189–200

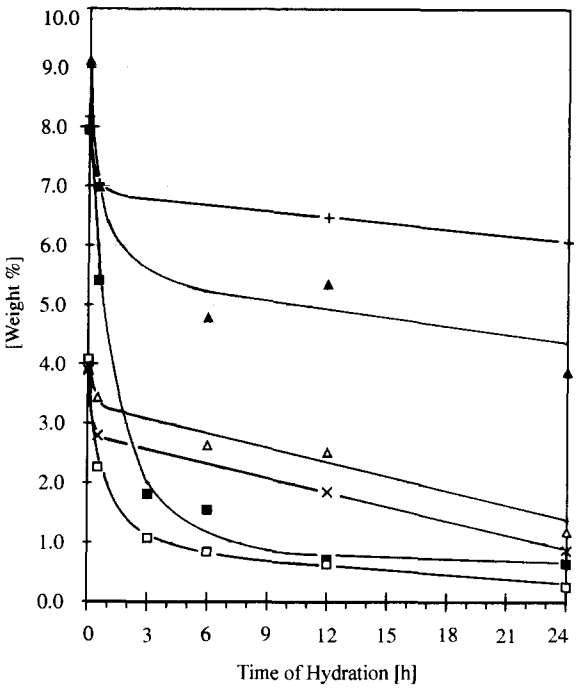


**FIGURE 2.** Comparison of the rates of $C_3A$ and ferrite dissolution during early hydration at water:cement ratio of 0.38 of cement pastes containing potassium carbonate (2-GfC), potassium carbonate, potassium citrate, and gypsum (2-PCG), and the admixture-free reference 2-REF. □, $C_3A$ and 2-PCG; △, $C_3A$ and 2-GfC; ×, $C_3A$ and 2-REF; ■, ferrite and 2-PCG; ▲, ferrite and 2-GfC; +, ferrite and 2-REF.

pastes (2-GfC), only the rate of dissolution of the ferrite phase is enhanced during the initial hydration period. Lignosulfonate interacts specifically with the aluminate phase, retarding its dissolution [7].

**DISSOLUTION OF THE ALITE PHASE.** The XRD results of the dissolution of the alite phase in 1-PCG and 1-REF cement pastes prepared with different water:cement (w:c) ratios during early and late hydration are given in Figure 3. The rate of alite dissolution is increased by the admixtures only during the initial hydration period. After 12 hours hydration at low w:c ratios, the dissolution rate is controlled by the w:c ratio.

## *Formation of Hydrous Products*

**CRYSTALLINE HYDROUS PRODUCTS.** In the samples containing citrate and carbonate solely or in combination as well as in the GfC samples, the main crystalline hydration product identified is an AFm phase [1] from the type $\{[Ca_2(Al_xFe_{1-x})(OH)_6]^+ [mY * nH_2O]^-\}$, Y being $OH^-$, $CO_3^{2-}$, $SO_4^{2-}$, $0 \leq n \leq 1$. The XRD reflection at 4.06–4.07 Å is detected only in the samples containing potassium carbonate consistent with a solid solution of carbonate ($Y = CO_3^{2-}$, $m \leq 0.5$) in the AFm phase [6]. A minimum crystallite size of 60–100 Å is estimated from the line width of the reflections. The highest yield of AFm phase is obtained when potassium carbonate is present. The incorporation of carbonate [10] stabilizes the AFm phase with respect to hydrogarnet. No hydrogarnets could be detected by XRD or by differential scanning calorimetry (DSC) [7]. The formation of the AFm phase coincides with the hardening of the citrate- and/or carbonate-containing cement pastes in the presence or absence of gypsum. Portlandite is formed in detectable amounts 2 to 3 hours after hardening; but in comparison with the reference samples, significantly less portlandite is formed in the citrate- and/or carbonate-containing samples. Other details are described elsewhere [7].

The XRD detection of the AFm and AFt phases, particularly ettringite, proved to be sensitive to the drying procedure, which caused line broadening and variations in the integral intensities of the AFm and AFt phases as reported previously [1,11,12].

Thus, to correlate the early kinetics of the dissolution of the clinker phases with the initial formation of hydrous products, in situ monitoring of hydration by XRD was used, similar to the procedure reported by Kuzel [11]. Due to the high finess of the cements studied, the in situ samples can be treated as wet powder samples. The water content remains constant as the polypropylene film cover prevents evaporation of water and contact with atmospheric carbon dioxide. However, the following limitations of the in situ XRD method have to be considered: (1) the X-rays penetrate only the surface layer of the sample (0.02 mm), therefore a high sample homogeneity is required; and (2) no corrections are possible for orientation effects or changes in the texture in the matrix. To prevent or minimize possible artefacts, a careful sample preparation with the optimum w:c ratio is essential and, as mentioned earlier, the cements studied have to be ground to sufficient fineness. The accuracy and resolution is limited by the recording time and is therefore significantly lower than for dry powders.

As an example, a partial section of the recorded in situ XRD patterns of the 1-PCG cement paste is shown in Figure 4. The results of the semiquantitative evaluations are presented in Figures 5 and 6. The results obtained with the reference samples (1-REF and 2-REF) are corroborated by the QXRD results and agree well with the common model for OPC hydration, hence they support the validity of the method. XRD patterns recorded in situ during the hydration of 1-PCG and 2-PCG show that after mixing with water an AFt phase is formed in significantly higher amounts than in the reference as a transient hydration product (Figure 4). The basal line at 9.58–9.60 Å is assigned to a "water deficient" ettringite $C_3A \cdot 3C\bar{S} \cdot H_{31}$ [13], assumed to be formed in low w:c pastes. Syngenite (9.52 Å) is

**TABLE 3.** Influence of potassium carbonate and potassium citrate on the rate of the dissolution of ferrite (series 1: C4AF, series 2: C4A1.1F0.9) in cement pastes (wt % of remaining ferrite)

| Time (days) | 1-REF (w:c = 0.38) | 1-PG (w:c = 0.26) | 1-CG (w:c = 0.26) | 1-PCG (w:c = 0.26) | 2-REF (w:c = 0.38) | 2-GfC (w:c = 0.38) | 2-PCG (w:c = 0.38) |
|---|---|---|---|---|---|---|---|
| 0 | 17.5 | 17.5 | 17.8 | 17.7 | 8.2 | 8.4 | 7.9 |
| 1 | 13.8 | 8.7 | 3.9 | 4.0 | 6.1 | 4.1 | 0.6 |
| 7 | 14.5 | 7.7 | 5.4 | 4.2 | 4.6 | 2.6 | 0.9 |
| 28 | 14.0 | 7.8 | 4.2 | 2.7 | 4.0 | 2.8 | 0.7 |

ruled out as its most intense lines at 3.16 Å (80%) and 2.86 Å (100%) are missing. Corroborating the QXRD results, the main hydration product is a hexagonal AFm phase. The line that can be correlated with hemicarboaluminate hydrate (4.07–4.10 Å) is stronger in the 1-PCG samples than in the 2-PCG samples. In both samples, 1-PCG and 2-PCG, significant amounts of arcanite (KS) are formed initially, which persist throughout the recorded hydration period.

The semiquantitative evaluations of the XRD patterns illustrate the transient nature of the AFt phase, formed in higher yield in the $C_3A$-free 1-PCG paste but with lower stability than in the 2-PCG paste (Figures 5 and 6). The XRD lines assigned to the AFm phase continue to grow long after the complete dissolution of the ferrite (2–3 hours) and aluminate phases (8 hours), leveling off after about 12 to 15 hours of hydration, indicating that the AFm phases are formed from an intermediary hydration product. The dependence of the onset of the AFm formation on the stability of the AFt phases, which in turn depends on the amount of gypsum added, suggests that in the presence of gypsum the intermediary product is the transient AFt phase [7]. Portlandite becomes visible in the XRD patterns only after the rate of AFm phase formation has diminished significantly. QXRD results show that significantly lower amounts of portlandite are formed in the PCG samples at equal w:c ratios, especially during early hydration (up to 12 hours) [7]. In reference samples, hardening coincides with the onset of alite dissolution and the emergence of portlandite.

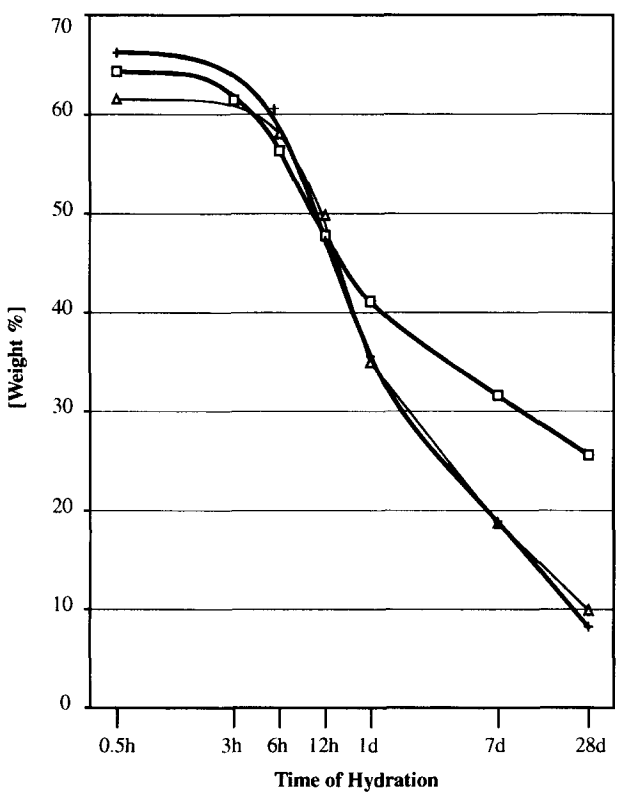


**FIGURE 3.** Influence of the w:c ratio on the rate of alite dissolution in potassium carbonate and potassium citrate containing samples (1-PCG) in comparison with the reference 1-REF. □, 1-PCG (w:c = 0.26); △, 1-PCG (w:c = 0.38); +, 1-REF (w:c = 0.38).

NONCRYSTALLINE HYDROUS PHASES. Environmental scanning electron microscope (ESEM) micrographs indicated the formation of large amounts of noncrystalline material with glassy-like appearance in 1-PCG and 2-PCG samples [7,9]. The fitted XRD background of the 28-day-old reference and 1-PCG samples (Figure 7) is enhanced to nearly the same extent at d-values usually associated with C-S-H (I)-gel [14] in agreement with the QXRD results (Figure 3). In the 1-PCG sample, an additional non-C-S-H-background enhancement is observed, visualized by the differential plot PCG-REF in Figure 7. The non-C-S-H-background is significantly higher in the citrate-containing samples and lower in the solely carbonate-containing samples [7].

The results of the evaluation of the background fitted with parabolas excluding contributions of microcrystalline materials are shown in Figures 8 and 9. The moderate decrease of crystallinity and the almost linear increase of the noncrystalline fraction on the logarithmic time scale in the reference (Figure 8) follows the rate and yield of alite dissolution (Figure 3) and water fixation [7]. The rapid decrease of the crystallinity in the 1-PCG sample during the initial 6 hours of sample hydration agrees well with the observed rapid dissolution of the ferrite phase, which is nearly complete within 3 to 6 hours. The noncrystalline fraction in the

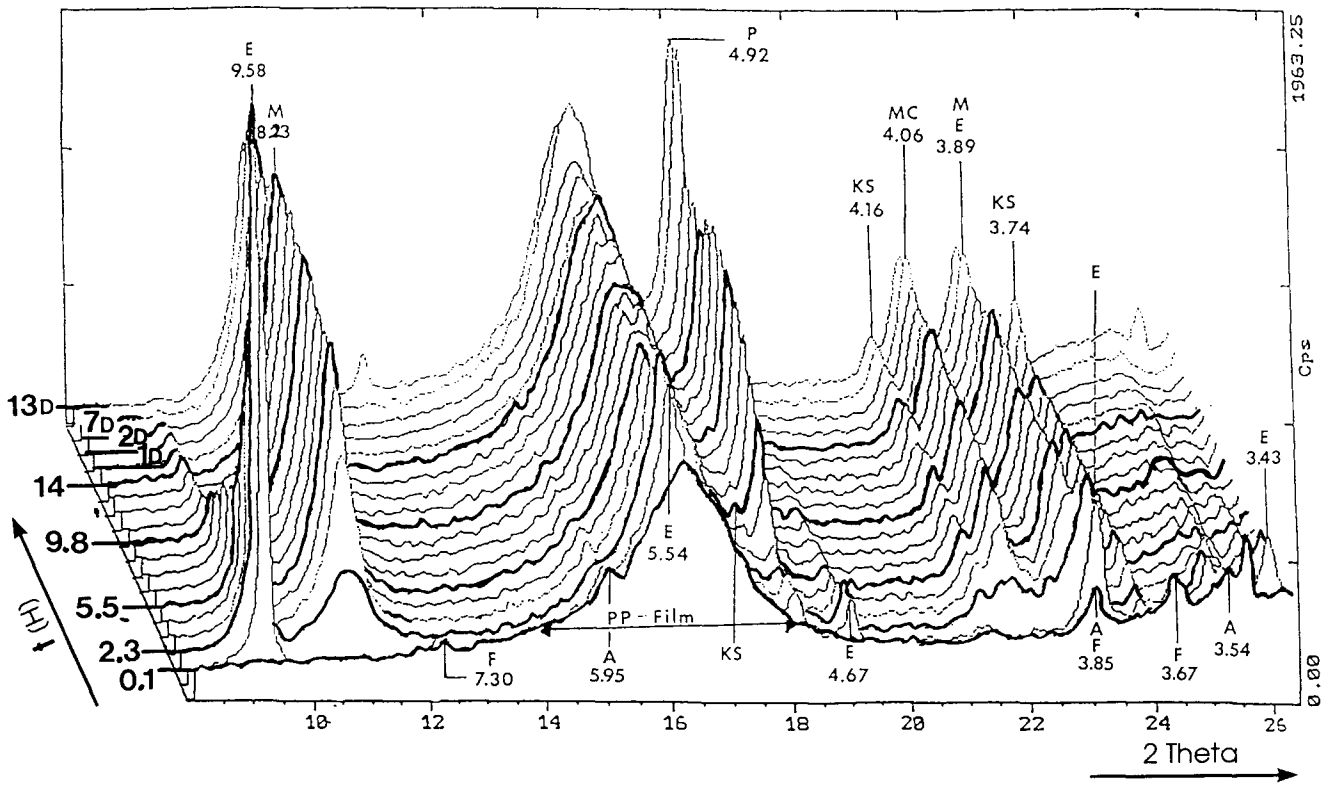


**FIGURE 4.** In situ recorded X-ray diffraction patterns during the hydration of 1-PCG. The patterns were recorded continuously up to 15 h and then discontinuously for the 19-hour, 24-hour, 42-hour, 7-day, and 13-day patterns. Denominations: alite (A), ferrite (F), AFm (M), hemicarboaluminate (MC), AFt (E), arcanite (KS), and Portlandite (P).

1-PCG sample increases rapidly up to 24 hours of hydration, further increase proceeds nearly at the same rate as in the reference congruent with the assumption that the rate of C-S-H gel formation during late hydration proceeds in both samples at about equal rates. The fraction of the noncrystalline phase formed is significantly higher in the citrate-containing samples—highest in the 1-PCG and lowest in the 1-GfC samples (Figure 9). From this, it is concluded that a significant fraction of hydrous products formed during early hydration in the presence of citrate (1-PCG) is noncrystalline and originates from hydration products of the ferro-aluminate phase.

## *Pore Solution Composition During Early Hydration*

The composition of the pore solution of 2-PCG and 2-REF cement pastes (w:c = 0.38) between 2 minutes and 24 hours after mixing with water was determined. Procedures and measuring conditions are reported elsewhere in detail [7,9]. Results are shown in Figure 10, the logarithmic time scale is divided into two sections, 0 to 30 minutes and 0.5 to 24 hours.

In the 2-PCG plots, the calcium concentration $Ca_{tot}$ comprises both free calcium ions and chelated calcium. Assuming that carbonate is removed from solution within minutes as calcium carbonate, then the measured carbon originates from citrate. Considering that citrate contains six carbon atoms, calcium and citrate are present in the pore solution in equimolar amounts, supporting the assumption that calcium is dissolved mainly as chelate. From the stability of the calcium citrate complex ($pK^{0,s}$ −4.86, pH 8) [15], the concentration of $Ca^{2+}_{(aq)}$ is estimated to be <1 mmol/L. From the solubility curve for C-S-H [16] for a concentration of 2–3 mmol/L $SiO_2$ (Figure 10), a saturation value for $Ca^{2+}_{(aq)}$ of 0.1–1.0 mmol/L is estimated. It is assumed that the low concentration of $Ca^{2+}_{(aq)}$ allows unusually high concentrations of aluminate and silicate anions. The extraordinary high values of dissolved Fe(III) are assumed to originate from $[Fe\text{-}cit_2]^{5-}$ [17].

## *Cementitious Properties—Properties of ISO-Mortar and Concrete*

In Table 4, results of ISO-mortar formulations with cements of series 1 ($C_3A$-free clinker) and series 2 (OPC clinker) are given. The admixture-containing formulations were tested at a w:c of 0.375 ± 0.005, except 1-PCG, which was too fluid for flow measurement at a

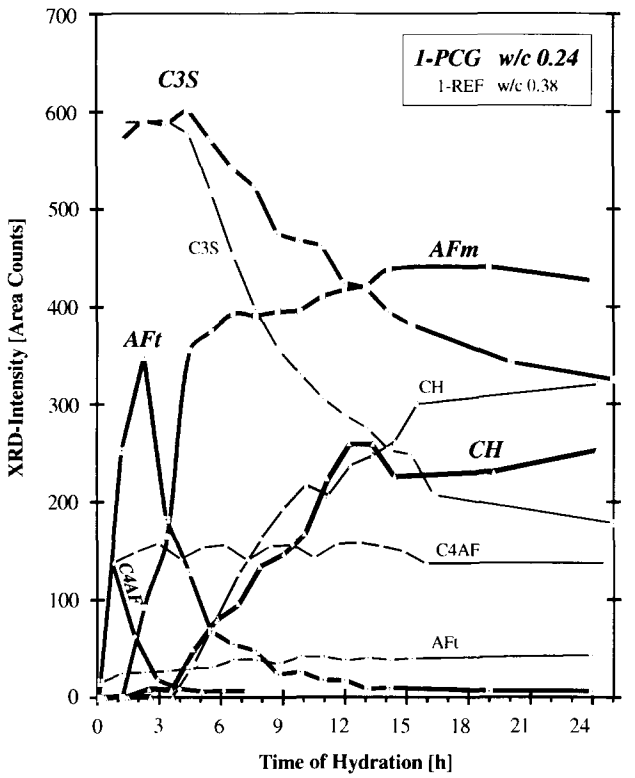


**FIGURE 5.** Semiquantitative evaluation of in situ recorded X-ray diffraction patterns during the hydration of 1-PCG at w:c = 0.24 and the reference 1-REF at w:c = 0.38.

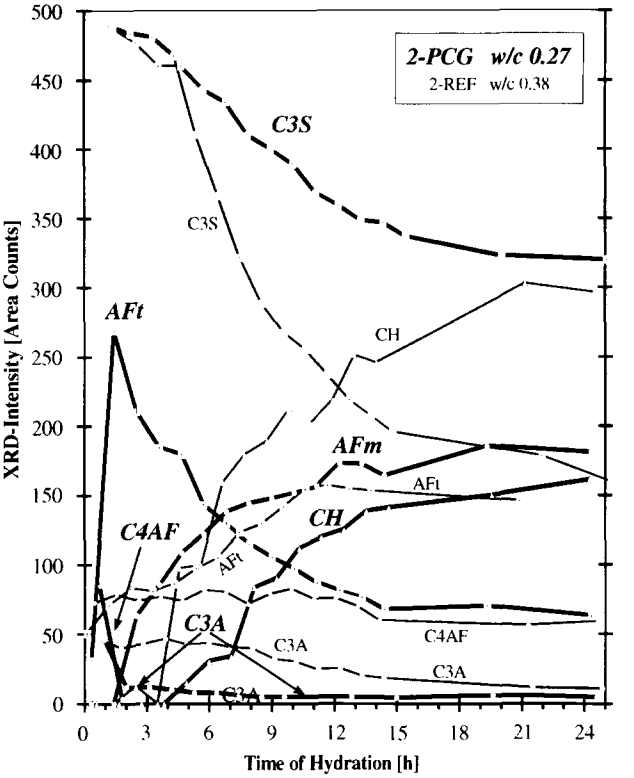


**FIGURE 6.** Semiquantitative evaluation of in situ recorded X-ray diffraction patterns during the hydration of 2-PCG at w:c = 0.27 and the reference 2-REF at w:c = 0.38.

w:c of 0.37. The 1-PCG and 2-PCG mortars were tested also at stiff and fluid consistencies; the reference was tested at standard consistency. In all formulations containing potassium carbonate and citrate solely or in combination, hardening starts with set in paste, mortar, and concrete. The set increases with the amount of gypsum added and may be adjusted between 2 minutes and 3 hours in the 2-PCG formulations. Results refer to formulations containing pure dihydrate. The influence of the gypsum phase on the cementitious properties of samples containing citrate is reported elsewhere [18].

With the type and the finess of clinkers studied, only low early strength values (2–3 MPa after 4–6 hours) are obtained with GfC formulations, whereas by replacing lignosulfonate (1-GfC) with citrate (1-PC), early strength increases by a factor of 4.5 (Table 4). Adding gypsum (1-PCG) increases strength further by about 10 to 20%. Citrate in combination with carbonate (1-PCG versus 1-CG) increases not only early strength but also late strength significantly.

In the 2-PCG concrete (w:c = 0.37), the initial strength gain of 20 MPa is attained within 1 hour after final set (2 hours). After a resting period of about 2 hours, strength increases again rapidly and continues to increase linearly on the logarithmic time scale.

# Discussion

## *Dissolution of the Clinker Phases*

In the common understanding of Portland cement hydration, the term hydration comprises both the hydration of the anhydrous phases and the formation of hydrous products. There is general agreement that in normal Portland cement pastes, dissolution of the clinker phases and precipitation of hydrous products occur nearly simultaneously. These reactions and several possible reaction mechanisms were extensively reviewed [1,2,19–21]. Most commonly, these solid hydrous products are assumed to form a diffusion barrier controlling further dissolution of the clinker particles. The dissolution of the aluminate and ferrite phases presumably is controlled by the formation of a protective layer consisting of amorphous or microcrystalline ettringite.

However, in the presence of citrate, the dissolution of the ferrite and aluminate phases occurs rapidly (Figures 1 and 2) and apparently is influenced neither by the formation nor by the disappearance of AFt phases during the initial hydration (Figures 5 and 6). From this, one might conclude that citrate prevents the formation of a protective AFt layer around the aluminate

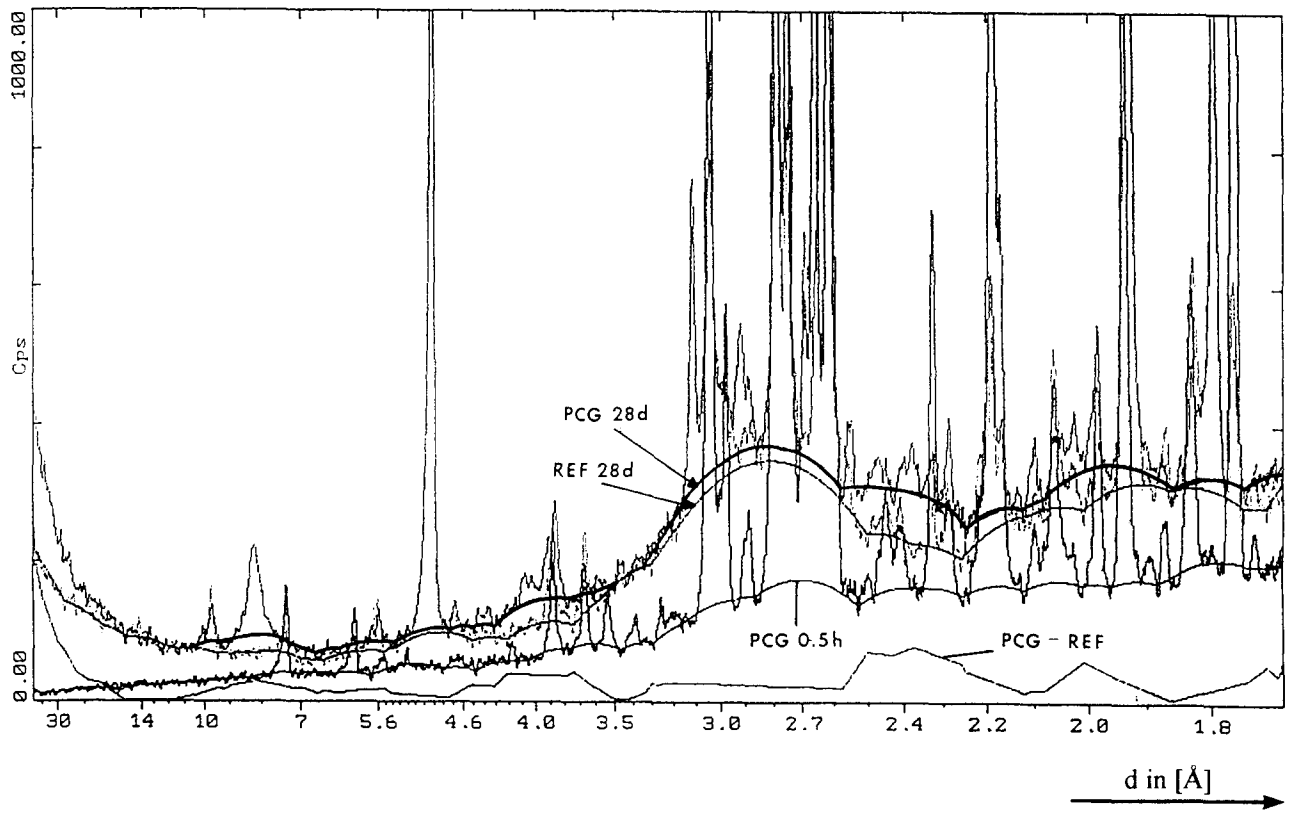


**FIGURE 7.** Fitted "structured" background of X-ray diffraction patterns of 0.5-hour- and 28-day-old 1-PCG (PCG) and 28-day-old 1-REF-samples (REF), both w:c = 0.38. Bottom line shows the difference between the backgrounds of 28-day-old 1-PCG and 1-REF samples.

and ferrite grains. This would imply that the AFt phase, formed during the initial hydration in significantly higher amounts in the 1-PCG and 2-PCG pastes than in the reference samples, is not protective. This would also imply that citrate intervenes on the level of ettringite formation, influencing ettringite morphology.

Citrate forms highly stable complexes with certain polyvalent metal cations [17,22,23]. With Fe(III), it forms complexes of the type $[Fe(Cit)_2]^{5-}$ [17], from which above pH 13 polymeric iron(III)-hydroxide-citrate precipitates rapidly [23]. The Fe (III) concentration in the pore solution of 2-PCG pastes is two orders of magnitude higher than in the reference (Figure 10). Following Gartner [6], this might increase the availability of Fe (III) for the incorporation in the hydration products. As only minor amounts of Fe(III) are known to be incorporated into ettringite [24], opposite to AFm phases [13], the specific enhancement of the rate of the ferrite dissolution by citrate is assumed to be due to the intervention of citrate on the level of the processes controlling the dissolution of the ferrite phases rather than on the level of the processes of product formation.

Addition of 0.2 to 0.4% of citric acid is reported to change the zeta-potential of cement pastes from positive to negative values indicating adsorption of citrate on the surface of the aluminate particles [25]. It was shown by Stumm [26] that the stability of surface complexes on hydrous oxide surfaces, for example, $\delta$-$Al_2O_3$ and $\alpha$-$Fe_2O_3$, is proportional to the stability of the corresponding complexes in solution. Contrary to Fe(III), Al(III) citrate complexes are not stable above pH 11 as $OH^-$ is a much stronger ligand for Al(III) than citrate [27]. Therefore, citrate will form stronger surface complexes with the Fe(III) than with the Al surface Lewis acid centers.

The specifically enhanced dissolution rate of the ferrite phase might then be explained by the ligand-promoted dissolution model developed by Stumm [26]. Bidentate ligands may form strong surface ring type chelates. Due to the *trans* effect, negative charge is transferred into the metal center, loosening the lattice metal oxygen bond and therefore promoting its dissolution.

The dissolution rate of ferrite in 1-PG (Figure 1) and in 2-GfC pastes (Figure 2) is significantly enhanced only during initial hydration until portlandite appears

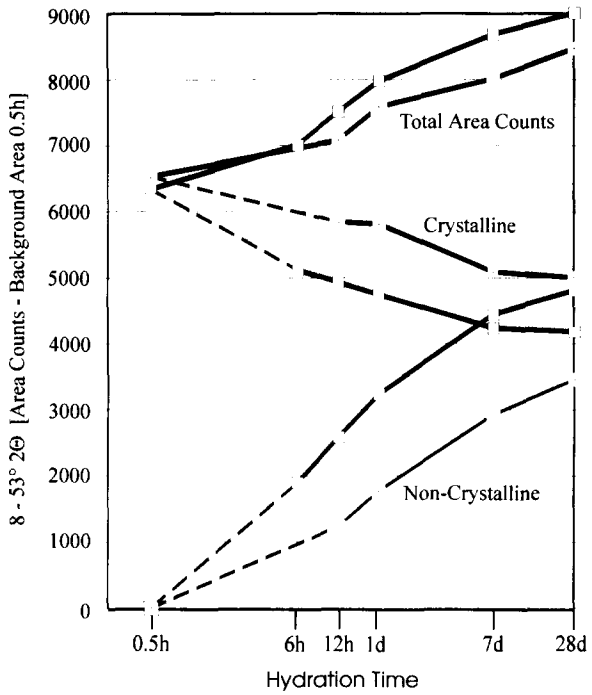


**FIGURE 8.** Repartition of crystalline and noncrystalline phases during the hardening of 1-PCG in comparison with the reference paste 1-REF at w:c = 0.38. □, 1-PCG; ×, 1-REF.

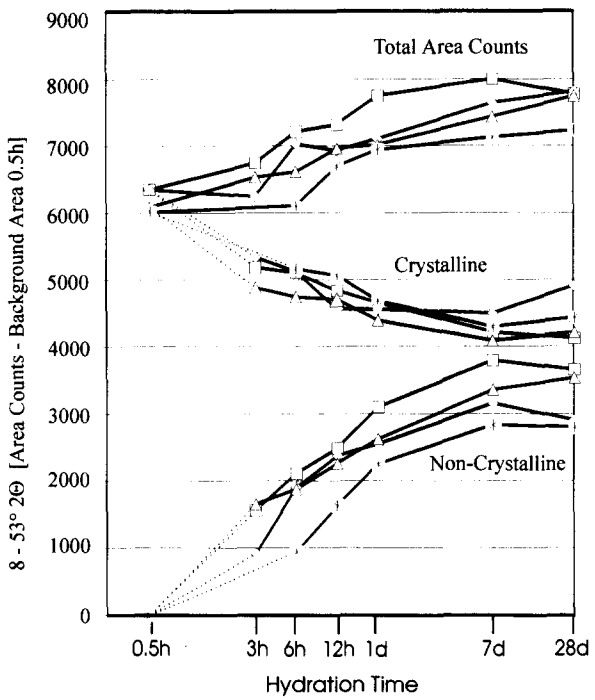


**FIGURE 9.** Influence of potassium citrate and potassium carbonate on the repartition of crystalline and noncrystalline phases during hardening at w:c = 0.26. □, 1-PCG; △, 1-PC; ◇, 1-PG; *, 1-GfC.

and the concentration of dissolved carbonate becomes negligible. Further dissolution proceeds at nearly the same rate as in the absence of admixtures (Table 3). The inhibition of further ferrite dissolution can hardly be explained by the formation of a protective ettringite layer in the 2-GfC pastes. In the 1-PG paste, ettringite formation is completely inhibited, in agreement with the phase diagram reported by Kuzel [11].

The validity of the protective layer hypothesis for the dissolution of the aluminate phases in the absence of sulfate is questioned by several authors [2,19]. In water, both aluminate [2,28] and ferrite [4,28] react within minutes, the reaction being complete within several hours. Portlandite [1,28] retards the aluminate and ferrite dissolution, the ferrite being significantly more sensitive than the aluminate. The hydrous products, mainly hexagonal and cubic calcium (ferro-) aluminate hydrates, either formed in the presence or absence of portlandite do not differ significantly [28,29]. The AFm phases formed during the early hydration of cement pastes containing carbonate and citrate do not influence the rate of aluminate and ferro-aluminate dissolution (Figures 5 and 6). This indicates that the hydrous products, especially AFm phases, do not form protective layers during the early stages of hydration.

If transport control is ruled out during the early hydration period, then inhibition has to be due to processes reducing the surface reactivity [26] of the aluminate and ferro-aluminate particles. Because most dissolution reactions of hydrous oxides as aluminium oxides, aluminium silicates, and silicates are surface controlled [26], these mechanisms might also apply to the dissolution of the aluminate and ferrite phases, as outlined in detail elsewhere [7] and originally proposed by Tadros et al. [30]. Surface complexation of calcium ions is assumed to stabilize the surface of clinker particles, especially of ferrites and aluminates. Sulfate enhances this effect [7,30] through formation of ternary surface complexes [26]. Excess sulfate, added as alkali sulfate, should accelerate the dissolution through ligand competition [26] by decreasing the concentration of $Ca^{2+}_{(aq)}$, which is actually observed [3,19]. Similarly, the initial enhancement of the rate of ferrite dissolution in the presence of large amounts of carbonate might also be due to the reduction of $Ca^{2+}_{(aq)}$ and the surface coverage with $Ca^{2+}$ [7]. The specific influence of potassium on the dissolution rate appears not to be very significant. This might be due to the relatively high alkali content already present in the clinkers studied.

Following the previous argumentation, the dissolution of alite is assumed to be controlled by the transport of excess calcium ions through C-S-H formed around the dissolving alite particles, leading to autoinhibition of the dissolution reaction [7]. This agrees

Advn Cem Bas Mat
1995;2:189–200

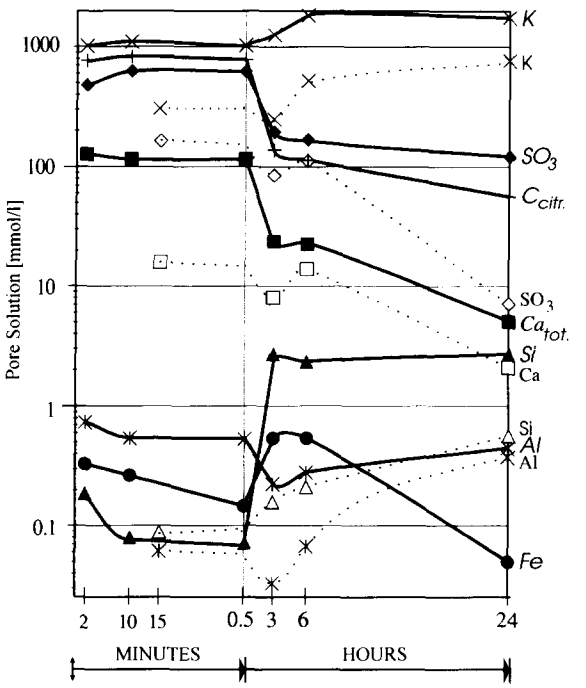


**FIGURE 10.** Concentrations in the pore solution of 2-PCG and 2-REF pastes at w:c = 0.38 (references 7 and 9). Thick lines correspond to values from 2-PCG pastes, dotted lines to values from 2-REF pastes. Fe concentration levels in 2-REF pastes (~10 μmol/L) are not shown.

well with the low sensitivity of the rate of the alite dissolution towards citrate and carbonate and the high sensitivity towards the w:c ratio (Figure 3) after the initial hydration period.

## *Hydrous Products versus Cementitious Properties*

The formation of solid hydrous products during the hydration of normal Portland cement pastes is assumed to occur by precipitation out of solution. For precipitation to occur, the solution has to be oversaturated with respect to the precipitating mineral phase [26,31]. In normal Portland cement pastes (2-REF), the pore solution is rapidly oversaturated with portlandite and saturated with gypsum (Figure 10). Therefore, dissolution of the clinker phases and precipitation of the hydrous products will occur nearly concurrently, as observed (Figures 5 and 6).

The admixture of carbonate and citrate changes the solution chemistry significantly as shown for the 2-PCG samples (Figure 10). During the plastic stage, within minutes, unusually high levels of sulfate, Fe, and Al are attained and calcium in solution is present mainly as citrate. Near the rapidly dissolving aluminate and ferrite particles, high concentrations of $Al(OH)_4^-$ and $Ca^{2+}_{(aq)}$ will develop micro-locally, oversaturated with respect to ettringite [32] at the interface with the pore solution high in sulfate. The amount and the stability of the AFt phase will depend mainly on the amount of aluminate and ferrite dissolved and the amount of gypsum added, similar to the mechanism proposed by Gartner [2,6], which assumes AFt/AFm conversion at the sulfate exhaustion point. The drop in the $C_{tot}$, sulfate, $Ca_{tot}$, and Al concentration coincides with the redissolution of the AFt phase and the rapid formation of AFm (Figures 5 and 6) and noncrystalline non-C-S-H phases (Figure 8). This might be interpreted to mean that significant amounts of citrate and sulfate are incorporated into the AFm and/or noncrystalline phases. Eventually, there might be an AFm solid solution composition with a minimum solubility even below the solubility of AFT phases. Gartner and Myers [6] reported the formation of low-sulfate AFm phases from the dissolution of ferrite accelerated by iron-complexing additives. Significant amounts of homogeneously distributed C-S-H might be formed throughout the solution during late hydration due to the high solution levels of silicate (Figure 10); this conclusion is supported by ESEM micrographs [7,9].

The strength development in mortar and concrete (Table 4) follows the two-step hydration of the clinker phases: the initial rapid strength increase coincides

**TABLE 4.** Cementitious properties of admixture containing portland cements in ISO-mortar and in concrete

| Formulation | 1-REF | 1-GfC | 1-PC | 1-PCG | | 2-REF | 2-GfC | 2-CG | 2-PCG | | 2-PCG Concrete |
|---|---|---|---|---|---|---|---|---|---|---|---|
| w:c | 0.45 | 0.37 | 0.37 | 0.31 | 0.34 | 0.48 | 0.38 | 0.38 | 0.34 | 0.37 | 0.37 |
| Flow (%) | 118 | 111 | 159 | 87 | 137 | 110 | 102 | 105 | 102 | 144 | 45–50 cm |
| Final Set (min) | 375 | 110 | 75 | 90 | 115 | 330 | 55 | 30 | 145 | 150 | 120 |
| Strength (MPa) | | | | | | | | | | | |
| 4 hours | 0.0 | 2.2 | | 16.9 | 13.7 | 0.0 | 2.4 | 5.5 | 14.9 | 12.1 | 20.1 |
| 6 hours | 0.0 | 2.9 | 13.1 | 20.2 | 16.2 | 0.0 | 2.9 | 9.7 | 15.6 | 13.6 | 23.2 |
| 24 hours | 18.8 | 36.0 | 39.7 | 50.8 | 45.2 | 24.1 | 31.7 | 20.9 | 36.9 | 33.0 | 46.5 |
| 7 days | 43.8 | 49.3 | 62.8 | 66.1 | 62.2 | 43.4 | 44.9 | 47.9 | 59.7 | 60.2 | 63.5 |
| 28 days | 62.0 | 60.0 | | | 81.5 | 56.0 | 57.0 | 56.3 | 72.8 | 72.3 | 76.6 |

with the formation of AFm and noncrystalline non-C-S-H phases, and the second step of strength increase coincides with the dissolution of alite and formation of C-S-H. However, the early strength development is not correlated with the amount of AFm phases but rather with the amount of noncrystalline non-C-S-H phases formed (Figure 9). The highest yields of crystalline AFm phases are formed in the solely carbonate-containing low early strength GfC and PG formulations, and the highest yields of noncrystalline non-C-S-H phases are formed in the high early strength citrate-containing formulations. The low sensitivity of early strength to the w:c ratio (Table 4) and the morphology of the hardened paste [7,9] indicates a gel-like structure [7]. The importance of the ferrite phase for the early strength development [33] implies that Fe(III) has a significant influence on the formation of the noncrystalline non-CSH phase. The iron(III)-hydroxide-citrate polymer formed from $[Fe(Cit)_2]^{5-}$ above pH 13 is reported to consist of spherical particles of diameter of 72 Å, the surface covered with citrate ligands, the core similar to the iron(III) hydroxide polymer formed in chelate-free alkaline solutions [23]. The inclusion of Al, present in solution as $Al(OH)_4^-$ and $[(OH)_3Al\text{-}O\text{-}Al(OH)_3]^{2-}$ [34], during the precipitation process is likely [35] analogous to calcium-ferro-hydrates in which Fe(III) is readily exchangeable with Al(III) [1,13]. Therefore, in the presence of citrate and sufficient ferrite, the formation of polymeric calcium-ferro-alumino-hydroxo-citrate particles in which Fe(III) provokes the polymeric structure is considered to be highly probable. Following Taylor [14], it might be closely admixed with C-S-H gel and AFm phases.

## Summary

The admixture of citrate and carbonate to Portland cements increases specifically the dissolution rate of the ferrite phase. In the presence of 1 to 3% potassium citrate, the ferrite phase dissolves nearly completely within 6 hours; carbonate has a much weaker effect during the initial hydration period. Citrate is assumed to act via surface complexation and ligand-promoted dissolution [26]. A reevaluation of the surface reaction control model [26], originally proposed by Tadros et al. [30] for the dissolution of aluminate, is suggested. In the presence of citrate, noncrystalline phases are generated in which iron(III)hydroxide presumably forms the polymeric backbone. In combination with carbonate, which stabilizes crystalline AFm areas, high early strength and increased late strength are obtained in mortar and concrete. The repartition of crystalline and noncrystalline hydrous materials is assumed to be an important factor in defining the cementitious properties.

## Acknowledgments

The author gratefully acknowledges comments from W. Stumm, ETH-Zurich; H.M. Jennings, Northwestern University; F.H. Wittman, ETH-Zurich; W. Schneider, ETH-Zurich; and U. Ludwig, RWTH-Aachen. The author also would like to express his thanks to R. Hausner, Veitsch-Radex-Central laboratories, for the great care with which XRD patterns were recorded and processed and for his very useful comments, to Holderbank Cement & Beton Rekingen and Bündner Cementwerke Union for financing the project, and to Holderbank Management and Consulting Ltd. for providing its facilities and technical support.

## References

1. Taylor, H.F.W. *Cement Chemistry;* Academic Press: London, 1991.
2. Gartner, E.M.; Gaidis, J.M. In *Materials Science of Concrete II;* Skalny, J.; Mindess, S.; Eds.; American Ceramic Society: Westerville, OH, 1991; pp. 9–40.
3. Tang, F.J.; Gartner, E.M. *Adv. Cem. Res.* **1988,** *1,* 67–74.
4. Carlson, E.T. *J. Res. NBS* **1964,** *68A,* 453–463.
5. Abdul-Maula, S.; Odler, I. *World Cement* **1982,** 216–222.
6. Gartner, E.M.; Myers, D. *J. Am. Ceram. Soc.* **1993,** *76,* 1521–1530.
7. Schwarz, W.; Sujata, K.; Jennings, H.M.; Gerdes, A.; Sadouki, H.; Wittmann, F.H. *Building Materials Reports No. 6,* Institute for Building Materials, ETH-Zürich/HIL: Zurich, Switzerland, 1994.
8. Klug, H.P.; Alexander, L.E. *X-Ray Diffraction Procedures;* Wiley: New York, 1974; pp. 356–534.
9. Sujata, K.; Schwarz, W.; Jennings, H.M. Submitted for publication.
10. Barret, P.; Bertrandie, D.; Beau, D. *Cem. Concr. Res.* **1983,** *13,* 789–800.
11. Kuzel, H.-J.; Meyer, H.W. *Hydration and Setting of Cements;* Nonat, A.; Mutin, J.C., Eds.; RILEM E. & F.N. Spon: London, 1992; pp. 137–150.
12. Odler, I.; Abdul-Maula, S. *Cem. Concr. Res.* **1984,** *14,* 133–141.
13. Schwiete, H.E.; Ludwig, U. *Proc. 5th Int. Symp. Chem. Cem.* **1968,** *2,* 33–77.
14. Taylor, H.F.W. *Z. Krist.* **1992,** *202,* 41–50.
15. Pearce, K.N. *Aust. J. Chem.* **1980,** *33,* 1511–1517.
16. Jennings, H.M. *J. Am. Ceram. Soc.* **1986,** *69,* 614–618.
17. Spiro, Th.G.; Bates, L.; Saltman, P. *J. Am. Chem. Soc.* **1967,** *89,* 5555–5559.
18. Schwarz, W. (Holderbank Financiere Glarus AG, Switzerland) *Patent Application* (28/12/90) WO 92/12103, US 07/923,427.
19. Jennings, H.M. *Advances in Cement Technology;* Ghosh, S.N., Ed.; Pergamon: Oxford, 1983; pp. 349–396.
20. Jennings, H.M.; Bhatty, J.I.; Hodson, S.K. *Advances in Cementitious Materials; Series Ceram. Trans. Vol. 16;* Mindess, S., Ed.; American Ceramic Society: Westerville, OH, 1985; pp 289–317.
21. Gartner, E.M.; Gaidis, J.M. *Materials Science of Concrete I;* Skalny, J., Ed.; American Ceramic Society: Westerville, OH, 1989; pp. 95–126.
22. Van Duin, M.; Peters, J.A.; Kieboom, A.P.G.; van Bekkum, H. *Recl. Trav. Chim. Pays-Bas* **1989,** *108,* 57–60.
23. Spiro, Th.G.; Pape, L., Saltman, P. *J. Am. Chem. Soc.* **1967,** *89,* 5559–5562.
24. Brown, P.W. *J. Am. Ceram. Soc.* **1987,** *70,* 493–496.

25. Singh, N.B.; Singh, A.K.; Prabha Singh, S. *Cem. Concr. Res.* **1986,** *16,* 911–920.
26. Stumm, W. *Chemistry of the Solid-Water Interface;* Wiley Interscience: New York, 1992.
27. Motekaitis, R.J.; Martell, A.E. *Inorg. Chem.* **1984,** *23,* 18–23.
28. Collepardi, M.; Monosi, S.; Moriconi, G.; Corradi, M. *Cem. Concr. Res.* **1979,** *9,* 431–437.
29. De Keyser, W.L.; Tenoutasse, N. *Proc. 5th Int. Symp. Chem. Cem.* **1968,** *2,* 379–386.
30. Tadros, M.E.; Jackson, W.Y.; Skalny, J. *Colloid and Interface Science IV;* Kerker, M., Ed.; Academic Press: New York, 1976; pp. 211–223.
31. Blum, A.E.; Lasaga, A.C. *Aquatic Surface Chemistry;* Stumm, W., Ed.; Wiley: New York; 1987; pp 255–292.
32. Zhang, F.; Zhou, Z.; Lou, Z. *7th ICCC* **1980,** *2,* 88–93.
33. Schwarz, W. (Holderbank Financiere Glarus AG, Switzerland) *Patent Application* (28/12/90) WO 92/12100, US 07/923,891.
34. Chang, B.T. *Bull. Chem. Soc. Jpn.* **1981,** *54,* 1960–1963.
35. Schneider, W. Private communication, June 1993.